Original Article

Microbial Biosystems 10(2) (2025) 2025.334380
10.21608/mb.2024.334380.1204

Contents lists available at Egyptian Knowledge Bank
Microbial Biosystems
Journal homepage: http://mb.journals.ekb.eg/

Phyto-synthesize of selenium nanoparticles via *Psidium guajava* leaves and study the efficacy versus Methicillin-Resistant *Staphylococcus aureus* (MRSA) and their biofilm

Zubydah K. Ibrahim, Halah H. Al-Haideri*

College of Science for Women, University of Baghdad. Department of Biology, Baghdad, Iraq.

ARTICLE INFO

Article history
Received 06 November 2024
Received revised 19 November 2024
Accepted 03 December 2024
Available online 01 June 2025

Corresponding Editors
Yousef, M.
Ibrahim, H.

Keywords
Biofilm inhibition,
cefoxitin resistance,
diabetic patients,
FTIR spectroscopy,
mecA gene,
Minimum inhibitory concentration (MIC).

ABSTRACT

Selenium nanoparticles (Se NPs) were generated using a green synthesis method utilizing *Psidium guajava* leaf extract (PGLE). By using FTIR, XRD, SEM, EDX, and DLS, Se NPs have been characterized. According to the results of characterization, Se NPs that have been combined with PGLE show homogenous NP surfaces, a clean appearance, and an average size of 187 nm. From 128 specimens collected from patients with diabetic type 1, only 29 were identified as *Staphylococcus* species, out of 29 isolates, 25 were identified as *S. aureus*, and 4 were other *Staphylococcus* species. MecA gene detection and the cefoxitin resistance pattern were used to identify methicillin-resistant *S. aureus* MRSA. Of the 25 isolates, 20 were identified as MRSA and 5 as MSSA. Twenty pathogenic MRSA strains were shown to be susceptible to phyto-synthesized SeNPs' antibacterial effects. In addition to demonstrating low MIC values ranging from 50 to 800 µg/mL, the results demonstrated that Se NPs exhibited promising antibacterial activities, with inhibition zones ranging from 12 ± 0.41 to 21.5 ± 0.85 mm. The capacity to form a strong biofilm was seen in only four of the twenty MRSA strains. In tests against four strains known to generate biofilms, the Se NPs proved to be effective. Biosynthesis of Se NPs by PGLE was successful, and these NPs showed promise as an antibacterial and antibiofilm agent against MRSA strains.

Published by Arab Society for Fungal Conservation

Introduction

Methicillin-resistant *Staphylococcus aureus* (MRSA) has emerged in various countries, presenting significant challenges to treatment due to its resistance to multiple therapeutic agents. *Staphylococcus* species are classified as coagulase-positive (CoPS) and coagulase-negative (CoNS) based on their ability to produce coagulase (Kamel et al. 2018; Lafta & Najem 2020). More than 80 species and subspecies of *Staphylococcus* have been identified on mucous membranes and the skin, often causing opportunistic infections and posing health risks (Atiyah & Alkhafaji 2020; Ahmed & Al-Daraghi 2022, Mokabel et al. 2024, Mohamed et al. 2025).

The treatment of MRSA is complicated by the emergence of multidrug-resistant strains that possess a staphylococcal cassette chromosome mec (SCCmec), a genetic element encoding proteins that confer resistance to β-lactam antibiotics. The mecA gene, carried on this mobile genetic element, is a key determinant of methicillin resistance (Lee et al. 2018). Initially, MRSA infections were treated with vancomycin in the late 1980s, which works by binding to the D-alanyl-D-alanine terminus of the bacterial peptidoglycan, thereby inhibiting cell wall

* *Corresponding author Email address*: halahm_bio@csw.uobaghdad.edu.iq (Halah H. Al-Haideri)

synthesis (Périchon & Courvalin 2009). This binding causes a conformational change that prevents precursor incorporation into the peptidoglycan chain, leading to cell wall degradation and lysis (Zhu et al. 2013).

In recent years, nanotechnology has emerged as a vibrant and multidisciplinary field (Soliman et al. 2023). Nanomaterials, due to their diverse physicochemical properties, have played a critical role in industrialization and are being applied in various cutting-edge sectors including agriculture and healthcare (Soliman et al. 2024). Among these, metal nanoparticles show significant potential due to their wide-ranging applications.

Nanoparticle biosynthesis involves reducing metallic ions into elemental nanoparticles through functional groups such as amines and alkanes found in metabolites like terpenoids, alkaloids, steroids, and flavonoids (Almuhayawi et al. 2024). Selenium nanoparticles (Se NPs) have garnered attention for their strong bioactivity and low toxicity, making selenium an essential mineral for human health (Ndwandwe et al. 2021). Selenium acts as a cofactor for antioxidant enzymes in humans, animals, and microbes (Zoidis et al. 2018). Biogenic Se NPs provide a safe and sustainable method of nanoparticle production without the need for harsh reducing or stabilizing agents (Kralova & Jampilek 2021).

Among various biosynthetic approaches, plant-mediated synthesis of Se NPs is gaining popularity due to its simplicity and ease of purification (Zambonino et al. 2021). Recent studies have successfully used different plant-based substances for Se NP production (Mulla et al. 2020; Hashem & Salem 2022). Natural products, including Se NPs, have been reported to possess antibacterial properties, some even showing activity against multidrug-resistant (MDR) bacteria (Shareef et al. 2022; Frankova et al. 2021). Antibacterial nanoparticles, such as those made from selenium, silver, gold, and zinc oxide, have demonstrated promising activity against MDR pathogens (Huang et al. 2019).

Psidium guajava (guava), a member of the Myrtaceae family, is known for its edible fruit and medicinal properties (Ojewole 2006). Guava leaves contain various bioactive compounds including flavonoids, alkaloids, glycosides, polysaccharides, steroids, and saponins (Nair & Chanda 2007). Quercetin, the major flavonoid in guava leaves, exhibits notable antibacterial, antioxidant, anti-inflammatory, and antiviral activities (Abramovič & Abram 2006).

In this study, *Psidium guajava* leaf extract (PGLE) was employed for the green synthesis of selenium nanoparticles as an eco-friendly and cost-effective method. The Se NPs were characterized using FTIR, XRD, SEM, EDX, and DLS techniques. Their antibacterial and antibiofilm activities were tested against 20 MRSA isolates, alongside the isolation and identification of these clinical strains.

Materials and Methods

Obtaining the leaf extract

The PGLE were collected from the garden of college Science for Women, University of Baghdad. After being gathered, the leaves were cut and allowed to dry in the shade for a period of four days. Following that, the extract from the leaves that had dried was powdered into a fine powder. Additionally, 100 mL of DH2O was mixed with 12 g of powdered leaf extract. A magnetic stirrer was subsequently utilized to maintain the mixture in the beaker at 60 °C for five hours. The derived extract was called P. guajava aqueous extract (Kumar et al. 2021). Se-NPs are synthesized using this extract.

Biosynthesis of SeNPs

After adding sodium selenite (Na2SeO3; 25 mM) to 100 mL of the guajava leaf extract that were generated, the optimal generation of Se NPs was achieved by adjusting the pH to 7.2, the temperature for incubation to 30 °C, and the reaction duration to 24 hours while being stirred at 120 rpm in an incubator that was shaking. The development of Se NPs was indicated by the hue changing to reddish orange. Centrifugal force at 10,000 rpm for 10 minutes was used to purify the produced Se NPs, then DW was used multiple times to get rid of any unattached biomolecules (Miglani & Tani-Ishii 2021).

Characterization of Se nanoparticles

Se-NPs were characterized by FT-IR spectrum assessment, which has a wavenumber ranging from 400 to 4000 cm−1. The KBr pellet approach was tested using the JASCO FT-IR 3600 Infra-Red spectrometer. The XRD-6000 lists, Shimadzu equipment, SSI, Japan, were used to evaluate the crystallization, crystallite size, and lattice of the produced Se NPs. The magnitude of the diffracted X-rays was calculated using the diffracted angle 2θ. The surface properties and fundamental of the generated Se-NPs (JEOL, JSM-6360LA, Tokyo, Japan) were assessed by SEM-EDX analysis. A sputter coater vacuum-coated gold after the generated Se-NPs were loaded onto holders. It was possible to assess the roughness of green-fabricated Se-NPs employing field-emitting scanning electron microscopy (SEM, Quanta FEG250). The hydrodynamic diameter, polydispersity index (PDI), and the predominant Se NP distribution of particle sizes were estimated using dynamic light scattering (DLS-PSS-NICOMP 380-USA)(El-Batal et al. 2020; Zaki et al. 2022; Soliman et al. 2023; Soliman et al. 2024).

Bacterial isolation and identification

One hundred and twenty-eight samples were collected from 15 March 2023 to the middle of June 2023 from urine and diabetic foot infections at the Medical City Department, National Center for Educational Laboratories, and Al-Kindey Hospital (ID:22/2007 on 25/05/2023). The samples were collected from different reference diabetic patients of all ages and genders. A total of 128 samples were collected and transported in sterilized transport medium containers. The samples were streaked on Mannitol salt agar (MSA) and incubated at 37°C for 24 hrs. Out of 128, 25 samples were identified as *S. aureus* by standard bacteriological methods tests that used colony morphology & mannitol fermentation, and biochemical tests using the VITEK2 system and 16S rRNA sequence analysis. All isolates were cultured routinely on MSA and Mueller-Hinton Broth (MHB) for growth culture. *S. aureus* reference strain ATCC700698 was purchased from American Type Culture Collection / US (Mohammed 2011)**.**

Antibiotic susceptibility test

To ascertain the impact of an antibiotic medication on *S. aureus* isolates and reference strains, the disc agar diffusion test was used. Briefly, clinical isolates were inoculated in pre-warmed MH broth, the growth was monitored to the mid of exponential phase (OD_{600} 0.5) and were streaked on MH agar plates. The following antibiotics were used: erythromycin (E) (15 µg), clindamycin (C) (2 µg), Tetracycline (TE) (30 µg), Cefoxitin (30 µg), trimethoprim-sulphamethoxazole (1.25/23.75 µg), gentamycin (10 µg), rifampicin (5 µg), ciprofloxacin (5 µg) and teicoplamin (30 µg).

Antibacterial assay of Se NPs

The antibacterial capability of generated **Se NPs** was evaluated in this study versus twenty MRSA strains, including codes (B1, B2, C4, C7, E3, A2, G8, F4, U6, S2, X1, K5, K3, F2, A22, C45, G87, C12, S23, and P6). Following being cultivated as a pure strain on MH broth, every type of microorganism under inquiry was evenly disseminated on sterilized petri dishes utilizing the agar diffusion well methods, which involves employing a clean cork borer to drill a 7 mm well on plates.

To evaluate the efficacy against bacteria, 100 µL of **Se NPs** were added to every well. The inhibited areas were then calculated after incubation period (Perez 1990; Humphries et al. 2018).

A plant extract of *Psidium guajava* leaves was used as a control, using sodium selenite as the first component. The plates had been incubated to a whole day at 37˚C. The following step was to measure the diameter of the area that developed surrounding each well when the incubation time ended. The broth-based microdilution technique was used to assess the generated **Se NPs** antibacterial effectiveness against the isolates. Thus, it enabled the computation of the MIC of Ss NPs. This experiment included the sequential dilution of selenium nanoparticles twice. **Se NPs** were supplemented with 10 µL of pure isolates, which is 0.5 McFarland. The collected specimens were subsequently kept at approximately 37˚C for 24 h (Humphries et al. 2018), the MIC would be determined to ascertain using a microplate reader (STATFAX, USA) and the smallest amount of the specimens being tested that inhibited the test organisms comparable to positive as well as negative controls (Abbey & Deak 2019).

Detection of biofilm producer isolates

As previously mentioned (Kamel et al. 2018), the tissue culture plate technique (TCP) was employed to detect the production of biofilms. ODc is the average OD of the negative control, while OD is the average OD of the MRSA isolates. The findings were interpreted as follows: non biofilm producer given that OD ≤ ODc, mild biofilm producer given that ODc < OD ≤2 ODc, moderate biofilm producer given that 2 ODc < OD ≤ 4 ODc, and strongly biofilm producer when 4 ODc < OD.

Antibiofilm assay

Throughout this work, the MTP technique was used to determine SeNPs' antibiofilm effectiveness. To attain an 0.5 McFarland, four biofilm-producing isolates were cultivated in 1 mL of LB broth medium at 37°C overnight. 100 µL of LB broth enriched with 1% glucose has been added to each well of a 96-well plate. After that, 0.1 mL of SeNPs (concentrations ranging from 800 to 25 µg/mL) as well as 0.01 mL of test broth strain solutions were added to the wells, and they underwent incubation for 48 hours at 37°C. Each well's media then carefully removed, and to get rid of any free-floating bacterial isolates, all wells were washed multiple times with 0.2 mL of phosphate-buffered saline. Test strain adhesion to the 96-well plate was stained using 1% (wt/vol) crystal violet staining. To get rid of extra stain, the 96-well plate was cleaned once more and let to dry. The biofilm mass was then destained for 20 minutes using 95% methanol. Each well was then filled with 0.25 ml of 30% glacial acetic acid to quantify the formation of biofilms. Finally, using a Tecan Elx800 microplate analyzer, the color was assessed at about 540 nm. We compared how the treated and uninfected holes performed (Soliman et al. 2023; Palanisamy et al. 2014).

Results

Characterization

FTIR examinations were utilized for detection several functional groups in the biomaterials that produce SeNPs

and cap/stabilize them. By contrasting the observed intensity bands with reference values, the functional groups were determined. Wave numbers at 3377, 2962, 2375, 1580, 1402, 1332, 1112, 856, 777, and 621 cm−1 suggest the relationship of a capping agent with SeNPs (Fig. 1).

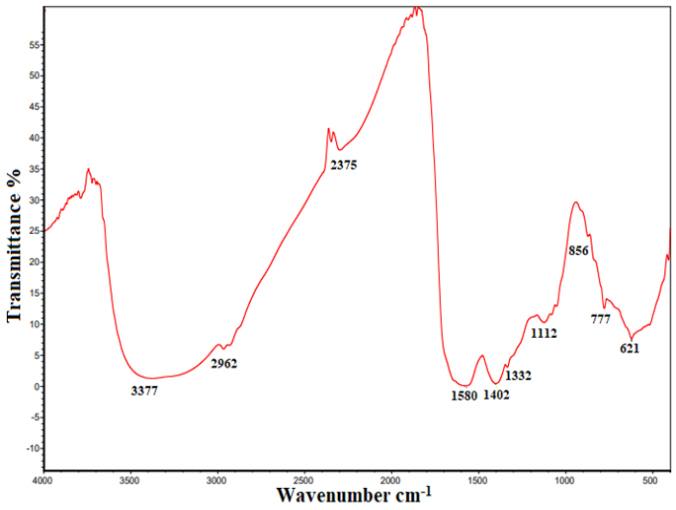

Fig. 1. Fourier-transform infrared (FTIR) spectrum of bio-fabricated selenium nanoparticles (Se NPs), illustrating the functional groups involved in the reduction and stabilization process.

The existence of alcohol and phenol is shown by the signal at 3377 cm−1. Existence of proteins is shown by the spectrum's peak at 1580 cm−1, which represents N–C and C–C stretching. The N–H stretch resonating observed in the proteins' amide bonds was identified as the source of the spectra at 1332 cm−1. The crosslinking of SeNPs with biomaterials produced by extracting *Psidium guajava* leaves was identified as the cause of the peak in the FT-IR portions of the synthesized SeNPs' spectra at 621 cm−1.

Figure 2 shows the XRD profile for SeNPs. XRD studies showed that the structure of SeNPs is monoclinic. Difraction peaks at 2=22.9° (100), 29.5° (101), 43.4° (110) and 52.4° (201) confirmed the crystalline structure of SeNPs. SEM pictures were used to assess the shape and surface characteristics of Se NPs.

The SeNPs' SEM picture, shown in figure 3, shows that their surfaces are homogenous and have a distinct look. When mixed and stabilized with the produced *Psidium guajava* leaf extract, Se NPs, which were normally separated as a rounded particle, appear as bright NPs. The fundamental structure as well as purity of the biosynthesized Se NPs were determined by EDX analysis, as shown in Fig. 4. Se NPs showed distinct selenium element absorption peaks at 1.40 keV. The spectra's abundance of selenium and absence of additional elemental peaks confirm the element's purity. The size of the particles along with the dispersion of the SeNPs were determined using DLS. Figure 5 shows that the SeNPs' average hydrodynamic diameter was 187 nm.

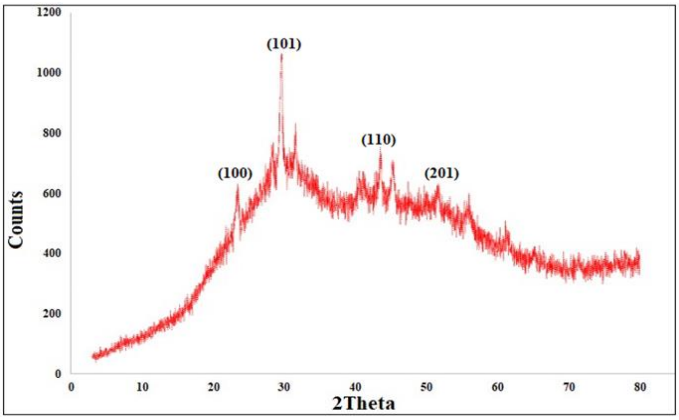

Fig 2. X-ray diffraction (XRD) pattern of bio-fabricated selenium nanoparticles (SeNPs), confirming their crystalline nature and phase purity.

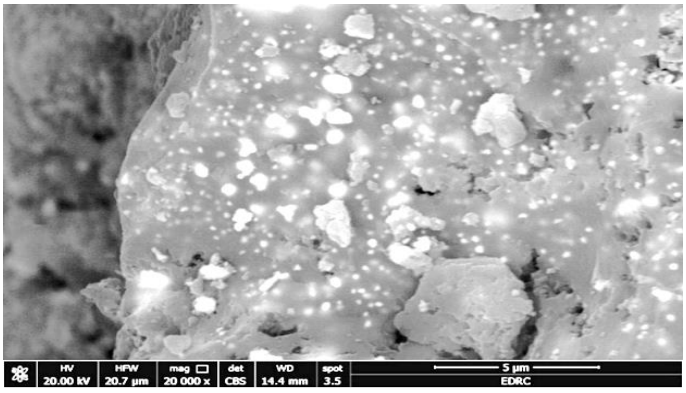

Fig 3. Scanning electron microscopy (SEM) image of bio-fabricated selenium nanoparticles (Se NPs), showing their surface morphology and particle size distribution.

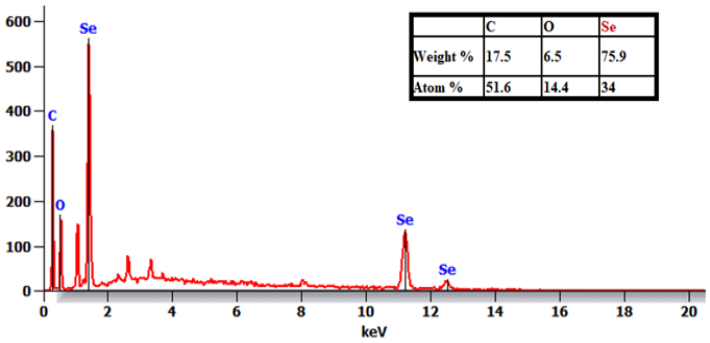

Fig 4. EDX spectrum of bio-fabricated Se-NPs confirming elemental composition.

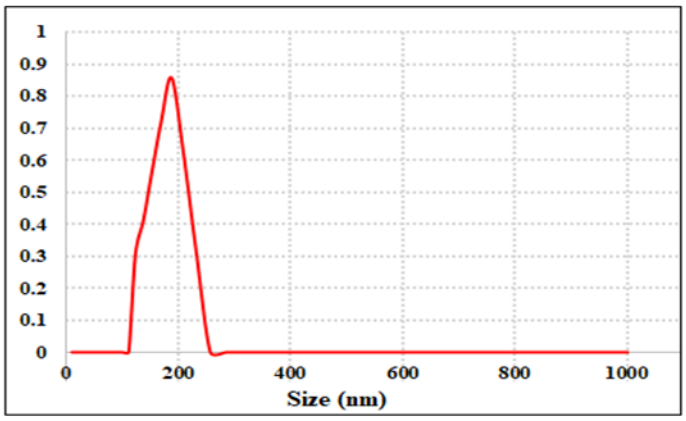

Fig 5. Dynamic light scattering (DLS) analysis of bio-fabricated Se-NPs showing particle size distribution.

Isolation and identification of S. aureus clinical isolates

Total of 128 specimens were collected from patients with diabetic type 1, from different hospitals in Baghdad, Iraq, and sources. Most samples were collected from diabetic foot and urine. Out of 128, only 29 were identified as *Staphylococcus* species, out of 29 isolates, 25 (86.2 %) were identified as *S. aureus*, and 4 (13.7 %) were other *Staphylococcus species*. The occurrence of *S. aureus* was higher in diabetic foot than from urine, among 25 isolates, 19 (76.0 %) were from diabetic foot, and 6 (24.0%) were from urine. Methicillin-resistant *S. aureus* MRSA was identified according to *mec*A gene detection and cefoxitin resistance pattern, a total of 25 isolates, 20 (80 %) were identified as MRSA, and 5 (20 %) were MSSA. In the diabetic foot, 14 (73.6 %) were MRSA, and 5 (26.3 %) were MSSA, 6 (100 %) from urine were MRSA (Table 1).

Antibiotic sensitivity assay

Disc diffusion assay was performed with nine selected antibiotics as CLSI (2022) recommended. The results showed that among 25 clinical isolates, all MRSA 20 (100 %) were resistant to gentamycin, erythromycin, cefoxitin, and Ciprofloxacin, whereas, 19 (95%) were resistant to teicoplanin, 18 (90.0 %) were resistance to tetracyclin, 16 (80.0 %), were resistance to rifampicin, and 17 (85.0%) were resistance to trimethoprim-sulphamethoxazole for both sources (Table 2).

Table 1 Clinical characteristics and distribution of methicillin-resistant *Staphylococcus aureus* (MRSA) isolates among diabetic patients.

Types of Specimens (total n=25)	MRSA (n=20) number (%)	MSSA (n=5) number (%)
Diabetic foot (n=19)	14 (73.6)	5 (26.3)
Urine (n=6)	6 (100)	0 (0.0)
Total	20	5

Table 2 Antimicrobial resistance patterns of clinical *Staphylococcus aureus* isolates.

Antibiotics µg ml^{-1}	Urine (MRSA) (n=6) number (%)	Diabetic Foot (MRSA) (n=14) number (%)	Total (n=20) number (%)
Gentamycin (10)	6 (100)	14 (100)	20 (100)
Erythromycin (15)	6 (100)	14 (100)	20 (100)
Teicoplanin (30)	5 (83.3)	14 (100)	19 (95.0)
Cefoxitin (30)	6 (100)	14 (100)	20 (100)
Tetracyclin (30)	6 (100)	12 (85.7)	18 (90.0)
Rifampicin (5)	5 (83.3)	11 (78.5)	16 (80.0)
Ciprofloxacin (5)	6 (100)	14 (100)	20 (100)
trimethoprim-sulphamethoxazole (1.25/ 23.75)	4 (66.6)	13 (92.8)	17 (85.0)

Antibacterial activity

Table 3 shows that the Se-NPs formed from the leaf extract of *Psidium guajava* have strong antibacterial properties in vitro. The majority of MRSA isolates showed a marked decrease in growth when exposed to Se-NPs. The mean IZD of the sensitive isolates ranged from 12 ± 0.41 to 21.5 ± 0.85 mm. It's interesting to note that the *Psidium guajava* leaf extract's acquired IZD for these isolates fell between 11 ± 0.5 and 13 ± 0.35 mm, suggesting that our extract had satisfactory efficacy versus the isolates that were tested. Table 1 quantitatively demonstrated the Se-NPs' inhibitory effects against the MRSA clinical isolates

at varying doses using the broth-based microdilution technique. The tested isolates' great sensitivity to the Se-NPs was shown by the low MIC values that were observed, which ranged from 50 to 800 µg/mL. Furthermore, six isolates had MIC values of 800 µg/mL at high concentrations, but only three isolates had the lowest MIC value. Furthermore, a variety of physiologically active phytochemical compounds, such as terpenoids, flavonoids, tannins, alkaloids, glycosides, and anthraquinones, may be primarily responsible for the Se-NPs' increased antibacterial capability.

Table 3. Antibacterial activity of bio-fabricated Se-NPs against MRSA isolates.

Character	Antibacterial activity of Se-NPs			
Isolates MRSA	IZD (mm) Plant extract	Sodium selenite	SeNPs	MIC µg/mL
B1	0	0	14 ± 0.58	600
B1	11 ± 0.5	0	18.5 ± 0.36	200
C4	0	0	12 ± 0.41	600
C7	0	0	0	800
E3	0	0	16.5 ± 0.74	400
A2	0	0	14.5 ± 0.24	600
G8	13 ±0.35	0	19.3 ± 0.65	100
F4	0	0	0	800
U6	0	0	18.9 ± 0.38	100
S2	12.5 ± 0.42	0	20.8 ± 0.81	50
X1	0	0	15.2 ± 0.44	400
K5	0	0	0	800
K3	0	0	0	800
F2	0	0	0	800
A22	0	0	19.3 ± 0.49	100
C45	12.1 ± 0.52	0	21.5 ± 0.85	50
G87	10.3± 0.45	0	19.5 ± 0.31	50
C12	0	0	12.9 ± 0.47	600
S23	0	0	0	800
P6	0	0	14.1± 0.22	400

Biofilm detection

Employing the microtitre plate method, the 20 bacterial isolates were examined for their capacity for producing biofilm. All twenty bacterial isolates (100%) were able to generate biofilm, according to the data. Four isolates (20%) were found to be strong biofilm generates, seven isolates (35%) to be moderate biofilm producers, and nine isolates (45%) to be weak biofilm creators when the amount of biofilm production of the isolated MRSA was assessed using a tissue culture test.

Biofilm inhibition activity

At concentrations 800 to 25 µg/mL the Se-NPs showed remarkable antibiofilm action against the strong biofilm producer MRSA isolates (C4, K5, F2 and S23). The Se-NP exhibited high significant inhibition of biofilm from 85% to 31% at the mentioned doses for F2 isolate, while the lowest inhibition against K5 isolate by 61% to 11% in dose dependent manner where the biofilm inhibition proportion was reduced to 73 % and 67% at 800 µg/mL for C4 and S23 (Fig 6).

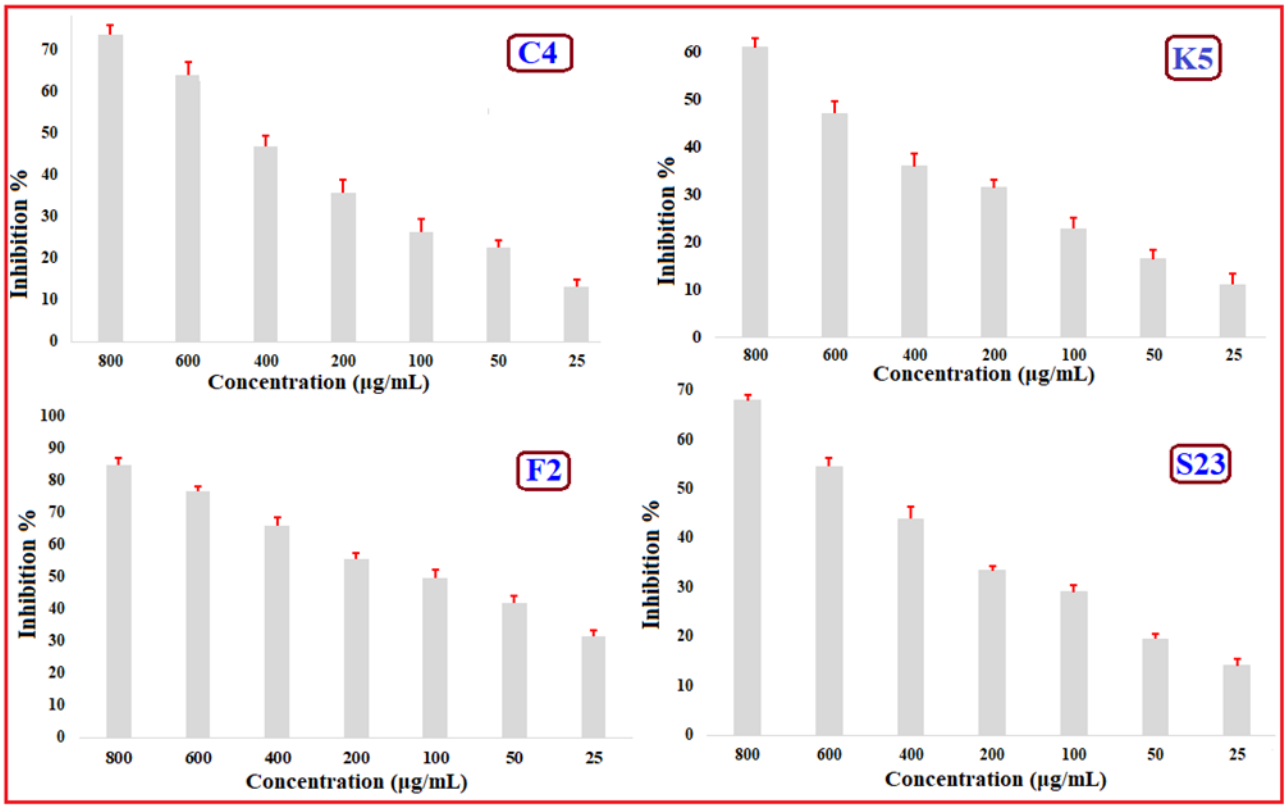

Fig 6. Antibiofilm activity of bio-fabricated Se-NPs against strong biofilm-producing MRSA isolates.

Discussion

Because of their many advantages—such as their low cost, practicality, and absence of hazards—biogenically generated nanomaterials have found application in a variety of industries, including biomedicine, electronics, and agriculture. its many advantages, such as their affordability, usefulness, and absence of risks (Chhipa 2019). The reducing effectiveness of P. guajava leaf extracts was used in the current study to generate SeNPs. This work demonstrated how *Psidium guajava* leaf extracts, including proteins, enzymes, and carbohydrates, may promote the biosynthesis of SeNPs, improving production, decreasing aggregation, and producing smaller dimensions of particles (Tuyen et al. 2023). When mixed with metallic precursors, the extract filtrate changed color, which was the first indication that nanoparticles were being biosynthesised. In many studies, plant leaf extract was used to generate SeNPs (Ropi et al. 2024).

FTIR was successfully examine the connections between Se NPs with P. guajava leaf extracts. P. guajava leaf extracts and SeNPs interacted as seen by different spectral bands at wavenumbers 856, 777, and 621 cm−1. The study's findings showed that various functional categories of organic compounds found in P. guajava leaf extracts affect the capping, stability, and reduction of Se-NPs. These materials consist of polysaccharides, amino acids, and enzymes (Puri et al. 2024). The amorphous morphology of the SeNPs produced by P. guajava leaf extracts has been demonstrated by the X-ray diffraction (XRD) data. The investigation's findings on the amorphous form of **Se NPs** are consistent with previous research on Pseudomonas stutzeri (Barabadi et al. 2018; Rajkumar et al. 2020). Furthermore, the external appearance of Se NPs appeared evident in the SEM picture, which shows homogeneous surfaces. It is evident that Se NPs were generally separated as rounded particles throughout the PGLE, resulting in dazzling NPs that were mixed and stabilized with the PGLE that were created (Sagar et al. 2024). An analytical method for analyzing the elements or chemical definition of the manufactured specimens is the EDX study (Amin et al. 2021). EDX analysis was used to assess the fundamental form and integrity of the biosynthesized Se NPs; the Se NPs had clear selenium element absorption peaks at 1.40 keV. The element's purity is confirmed by the spectra's abundance of selenium and lack of other elemental peaks(Piacenza et al. 2021). The study of dynamic light scattering (DLS) is an essential method for figuring out the measurement as well as distribution of NPs inside colloidal fluids. The mean size of the SeNPs generated in this work was found to be 187 nm using DLS analysis. To evaluate the similarity or heterogeneity of the colloidal nanoparticles, the scientists employed the polydispersity index (PDI) statistic (Fouda et al. 2021).

In our research, the resistance pattern of MRSA was variable according to the source of isolation. In general, all MRSA isolates 100 % were completely resistant to gentamycin, erythromycin, cefoxitin, tetracycline, and ciprofloxacin, our results are consistent with the result of (Yousefi et al. 2016; Anwar et al. 2020). In addition, 95.0 % of MRSA isolates showed a pattern of resistance toward Teicoplanin, which is agreed with (Kumari et al. 2016; Kot et al. 2020). According to microbiological measurements of the inhibition zone widths, the application of SeNPs bio fabricated from P. guajava leaf extracts clearly had an inhibitory impact. With inhibition zones ranging from 12 ± 0.41 to 21.5 ± 0.85 mm, the SeNPs showed antibacterial actions against MRSA isolates. These findings suggest that one potential mechanism underlying the antibacterial action of Se NPs is the generation of reactive oxygen species (ROS) (Yang et al. 2019; Madkour 2020). interruption of cell survival mechanisms as well as passage of nanoparticles into cells. ROS generated by nanomaterials are essential for apoptosis and cellular damage. ROS generation encourages oxidative DNA damage, which results in cell wall breakdown and cellular content release (Nguyen et al. 2017), According to reports, Se NPs have antibacterial properties versus E. coli O157:H7, and *Staphylococcus aureus*. Se NPs work by altering osmotic equilibrium or breaking down specific vital biochemical connections in the membrane to inhibit bacterial growth and avoid the development of biofilms (Xu et al. 2020). The antibacterial action mechanism was determined by the dispersion of NPs among the microorganisms and their non acidic propensity (Ghobashy et al. 2022).

The ability of the MRSA to form biofilm was confirmed by the use of microtiter plate evaluations. When compared to the planktonic state, the formation of biofilms by the culture is clearly evident. Metabolic resistance in methicillin-resistant *Staphylococcus aureus* (MRSA) is mostly shown by the formation of biofilms (Garrett et al. 2008; Selvaraj et al. 2019). The biofilm matrix prevents the antimicrobial agent from diffusing. The change in the biological processes of the bacteria within the biofilm provides resistance to the medications in along with diffusion (Craft et al. 2019). The SeNPs demonstrated their capacity to prevent the MRSA from forming biofilms. In previous study documented that using SeNPs in conjunction with antibacterial chemicals disrupts the biofilms of drug-resistant *S. aureus* and lowers the antibiotics' MICs (Cihalova et al. 2015; Zonaro et al. 2015). Following treatments with silver nanoparticles, intracellular contents were seen to be released from *S. aureus* and *P. aeruginosa*, respectively. They also suggested that the nanomaterial disrupted biofilms by deregulating cell-to-cell adhesion. According to a different research, biofilms were inhibited by inhibitory quantities of silver nanoparticles because they significantly reduced Klebsiella pneumoniae's synthesis of EPS (Goswami et al. 2015; Mapara et al. 2015). It was showed that *Proteus mirabilis*, *P. aeruginosa*, and *S. aureus* biofilms were suppressed by SeNPs (Siddique et al. 2020; Shakibaie et al. 2015).

Conclusion

Psidium guajava leaf extract (PGLE) facilitated the biosynthesis of monometallic selenium nanoparticles (Se NPs), which were subsequently characterized using FTIR, XRD, SEM, EDX, and DLS techniques. Bioactive phytochemicals from plant extracts function as capping agents, inhibiting the aggregation of nanoparticles and altering their biological activity. At 187 nanometers. Our findings indicate that Se NPs exhibit antibacterial efficacy against clinical MRSA isolates at a concentration of 800 µg/mL. Results indicate that Se NPs exhibited significant anti-biofilm activity against four isolates known for their robust biofilm production. SeNPs may provide advantages for various pharmacological applications.

Conflict of Interest:

The author declare that they have no conflict of interest.

Funding

No governmental, commercial, or nonprofit funding agencies provided any funds for this project.

References

Abbey TC, Deak E. (2019). 'What's new from the CLSI subcommittee on antimicrobial susceptibility testing M100', *Clinical Microbiology Newsletter*, 41: 203-09.

Abramovič H, Abram V. (2006). 'Effect of added rosemary extract on oxidative stability of Camelina sativa oil', *Acta agriculturae Slovenica*, 87: 225-61.

Ahmed ZF, Al-Daraghi WAH. (2022). 'Molecular detection of medA virulence gene in Staphylococcus aureus isolated from Iraqi patients', *Iraqi journal of biotechnology*, 21.

Almuhayawi MS, Alruhaili MH, Soliman MKY, Tarabulsi MK, Ashy RA, Saddiq AA, Selim S, Alruwaili Yr, Salem SS. (2024). 'Investigating the in vitro antibacterial, antibiofilm, antioxidant, anticancer and antiviral activities of zinc oxide nanoparticles biofabricated from Cassia javanica', *Plos one*, 19: e0310927.

Amin MA, Ismail MA, Badawy AA, Awad MA, Hamza MF, Awad MF, Fouda A. (2021). 'The Potency of fungal-fabricated selenium nanoparticles to improve the growth performance of Helianthus annuus L. and

control of cutworm Agrotis ipsilon', *Catalysts*, 11: 1551.

Anwar K, Hussein D, Salih J. (2020). 'Antimicrobial susceptibility testing and phenotypic detection of MRSA isolated from diabetic foot infection', *International Journal of General Medicine*: 1349-57.

Atiyah AS, Alkhafaji MH. (20200. 'Isolation of Enterococcus Species from Food Sources and Its Antibacterial Activity against *Staphylococcus aureus'*, *Iraqi Journal of Science*: 3164-71.

Barabadi H, Kobarfard F, Vahidi H. (20180. 'Biosynthesis and characterization of biogenic tellurium nanoparticles by using Penicillium chrysogenum PTCC 5031: A novel approach in gold biotechnology', *Iranian journal of pharmaceutical research: IJPR*, 17: 87.

Chhipa H. (2019). 'Mycosynthesis of nanoparticles for smart agricultural practice: a green and eco-friendly approach.' in, *Green synthesis, characterization and applications of nanoparticles* (Elsevier).

Cihalova K, Chudobova D, Michalek P, Moulick A, Guran R, Kopel P, Adam V, Kizek R. (2015). *'Staphylococcus aureus* and MRSA growth and biofilm formation after treatment with antibiotics and SeNPs', *International Journal of Molecular Sciences*, 16: 24656-72.

Craft KM, Nguyen JM, Berg LJ, Townsend SD. (2019). 'Methicillin-resistant *Staphylococcus aureus* (MRSA): antibiotic-resistance and the biofilm phenotype', *MedChemComm*, 10: 1231-41.

El-Batal AI, Mosallam FM, Ghorab MM, Hanora A, Gobara M, Baraka A, Elsayed MA, Pal K, Fathy RM, Abd Elkodous M. (2020). 'Factorial design-optimized and gamma irradiation-assisted fabrication of selenium nanoparticles by chitosan and Pleurotus ostreatus fermented fenugreek for a vigorous in vitro effect against carcinoma cells', *International journal of biological macromolecules*, 156: 1584-99.

Fouda A, Hassan SE, Saied E, Azab MS. (2021). 'An eco-friendly approach to textile and tannery wastewater treatment using maghemite nanoparticles (γ-Fe2O3-NPs) fabricated by Penicillium expansum strain (Kw)', *Journal of Environmental Chemical Engineering*, 9: 104693.

Frankova ALV, Merinas-Amo T, Leheckova Z, Doskocil I, Soon JW, Kudera T, Laupua F, Alonso-Moraga A, Kokoska L. (2021). 'In vitro antibacterial activity of extracts from Samoan medicinal plants and their effect on proliferation and migration of human fibroblasts', *Journal of Ethnopharmacology*, 264: 113220.

Garrett TR, Bhakoo M, Zhang Z. (20080. 'Bacterial adhesion and biofilms on surfaces', *Progress in natural science*, 18: 1049-56.

Ghobashy MM, Soliman YS, Soliman MAW, El-Sayyad GS, Abdel-Fattah AA. (2022). 'Radiation synthesis and in vitro evaluation of the antimicrobial property of functionalized nanopolymer-based poly (propargyl alcohol) against multidrug-resistance microbes', *Microbial pathogenesis*, 172: 105777.

Goswami SR, Sahareen T, Singh M, Kumar S. (2015). 'Role of biogenic silver nanoparticles in disruption of cell–cell adhesion in Staphylococcus aureus and Escherichia coli biofilm', *Journal of Industrial and Engineering Chemistry*, 26: 73-80.

Hashem AH, Salem SS. (2022). 'Green and ecofriendly biosynthesis of selenium nanoparticles using Urtica dioica (stinging nettle) leaf extract: Antimicrobial and anticancer activity', *Biotechnology journal*, 17: 2100432.

Huang T, Holden JA, Heath DE, O'Brien-Simpson NM, O'Connor AJ. (2019). 'Engineering highly effective antimicrobial selenium nanoparticles through control of particle size', *Nanoscale*, 11: 14937-51.

Humphries RM, Ambler J, Mitchell SL, Castanheira M, Dingle T, Hindler JA, Koeth L, Sei K. (2018). 'CLSI methods development and standardization working group best practices for evaluation of antimicrobial susceptibility tests', *Journal of clinical microbiology*, 56: 10.1128/jcm. 01934-17.

Kamel Z, Helmy NAM, Soliman MKY, Mashahit MA. (2018). 'Impact of biofilm production in methicillin resistant *Staphylococcus aureus* among diabetic foot patient', *Egyptian Journal of Medical Microbiology*, 27: 93-98.

Kot B, Wierzchowska K, Piechota M, Grużewska A. (2020). 'Antimicrobial resistance patterns in methicillin-resistant *Staphylococcus aureus* from patients hospitalized during 2015–2017 in hospitals in Poland', *Medical Principles and Practice*, 29: 61-68.

Kralova, K, Jampilek J. (2021). 'Responses of medicinal and aromatic plants to engineered anoparticles', *Applied Sciences*, 11: 1813.

Kumar M, Tomar M, Amarowicz R, Saurabh V, Nair MS, Maheshwari C, Sasi M, Prajapati U, Hasan M, Singh S. (2021). 'Guava (*Psidium guajava* L.) leaves: Nutritional composition, phytochemical profile, and health-promoting bioactivities', *Foods*, 10: 752.

Kumari J, Shenoy SM, Baliga S, Chakrapani M, Bhat GK. (2016). 'Healthcare-Associated Methicillin-Resistant *Staphylococcus aureus*: Clinical characteristics and antibiotic resistance profile with emphasis on macrolide-lincosamide-streptogramin B resistance', *Sultan Qaboos University Medical Journal*, 16: e175.

Lafta IJ, Najem MJ. (2020). 'Characterization of Mannitol fermenter and salt Tolerant Staphylococci from breast

tumor biopsies of Iraqi women', *Baghdad Science Journal*, 17: 0415-15.

Lee AS, Lencastre HD, Garau J, Kluytmans J, Malhotra-Kumar S, Peschel As, Harbarth S. (2018). 'Methicillin-resistant *Staphylococcus aureus'*, *Nature reviews Disease primers*, 4: 1-23.

Madkour LH. (2020). *Reactive oxygen species (ROS), nanoparticles, and endoplasmic reticulum (er) stress-induced cell death mechanisms* (Academic Press).

Mapara N, Sharma M, Shriram V, Bharadwaj R, Mohite KC, Kumar V. (2015). 'Antimicrobial potentials of Helicteres isora silver nanoparticles against extensively drug-resistant (XDR) clinical isolates of Pseudomonas aeruginosa', *Applied microbiology and biotechnology*, 99: 10655-67.

Miglani S, Tani-Ishii N (2021). 'Biosynthesized selenium nanoparticles: Characterization, antimicrobial, and antibiofilm activity against Enterococcus faecalis', *PeerJ*, 9: e11653.

Mohammed SM. (2011). 'Use of Cefoxitin as indicator for detection of Methicillin Resistant *Staphylococcus aureus'*, *Baghdad Science Journal*, 8: 947-55.

Mohamed A, Mohamed A K, Zahran A, Gad A, Mekky A. (2025). Antimicrobial, anti-inflammatory, anticancer and antiviral activity of bioactive compounds from Pseudomonas aeruginosa isolated from Mediterranean Sea, Alexandria, Egypt. *Microbial Biosystems,* 10(1), 123-134. doi: 10.21608/mb.2025.322359.1173

Mokabel A, Gebreel H, Youssef H, El-Kattan N, Abdel-Wahhab M. (2024). Prevalence of multidrug resistant bacteria in Egyptian hospitalized patients. Microbial Biosystems, 9(2), 121-132. doi: 10.21608/mb.2024.312767.1147

Mulla NA, Otari SV, Bohara RA, Yadav HM, Pawar SH. (2020). 'Rapid and size-controlled biosynthesis of cytocompatible selenium nanoparticles by Azadirachta indica leaves extract for antibacterial activity', *Materials Letters*, 264: 127353.

Nair R, Chanda S. (2007). 'In-vitro antimicrobial activity of *Psidium guajava* L. leaf extracts against clinically important pathogenic microbial strains', *Brazilian Journal of Microbiology*, 38: 452-58.

Ndwandwe BK, Malinga SP, Kayitesi E, Dlamini BC. (2021). 'Advances in green synthesis of selenium nanoparticles and their application in food packaging', *International Journal of Food Science & Technology*, 56: 2640-50.

Nguyen THD, Vardhanabhuti B, Lin M, Mustapha A. (2017). 'Antibacterial properties of selenium nanoparticles and their toxicity to Caco-2 cells', *Food Control*, 77: 17-24.

Ojewole JA. (2006). 'Antiinflammatory and analgesic effects of *Psidium guajava* Linn.(Myrtaceae) leaf aqueous extract in rats and mice', *Methods and findings in experimental and clinical pharmacology*, 28: 441-46.

Palanisamy NK, Ferina N, Amirulhusni AN, Mohd-Zain Z, Hussaini J, Ping LJ, Durairaj R. (2014). 'Antibiofilm properties of chemically synthesized silver nanoparticles found against Pseudomonas aeruginosa', *Journal of Nanobiotechnology*, 12: 1-7.

Perez C. (1990). 'Antibiotic assay by agar-well diffusion method', *Acta Biol Med Exp*, 15: 113-15.

Périchon B, Courvalin P. (2009). 'VanA-type vancomycin-resistant *Staphylococcus aureus'*, *Antimicrobial agents and chemotherapy*, 53: 4580-87.

Piacenza E, Presentato A, Ferrante F, Cavallaro G, Alduina R, Martino DFC. (2021). 'Biogenic selenium nanoparticles: a fine characterization to unveil their thermodynamic stability', *Nanomaterials*, 11: 1195.

Puri A, Mohite P, Ansari Y, Mukerjee N, Alharbi HM, Upaganlawar A, Thorat N. (2024). 'Plant-derived selenium nanoparticles: investigating unique morphologies, enhancing therapeutic uses, and leading the way in tailored medical treatments', *Materials Advances*, 5: 3602-28.

Rajkumar K, Mvs S, Koganti S, Burgula S. (2020). 'Selenium nanoparticles synthesized using Pseudomonas stutzeri (MH191156) show antiproliferative and anti-angiogenic activity against cervical cancer cells', *International journal of nanomedicine*: 4523-40.

Ropi NAM, Abd Aziz N Yeng LH, Kai CK. (2024). 'Green Synthesis of Selenium Nanoparticles Using Leaves Extract of *Psidium guajava'*, *Innovation Centre in Agritechnology for Advanced Bioprocessing (ICA) Universiti Teknologi Malaysia Pagoh Campus Johor Darul Takzim, Malaysia*: 34.

Sagar S, Jeyaraj G, Ohri T, Shirlal S, Sandhu H, Kaur R. (2024). 'Green Synthesis of Selenium Nanoparticles Mediated Aqueous extract of Euphorbia Tirucalli and its Antimicrobial and Cytotoxic Activities', *African Journal of Biomedical Research*, 27: 1035-42.

Selvaraj A, Jayasree T, Valliammai A, Pandian SK. (2019). 'Myrtenol attenuates MRSA biofilm and virulence by suppressing sarA expression dynamism', *Frontiers in microbiology*, 10: 2027.

Shakibaie M, Forootanfar H, Golkari Y, Mohammadi-Khorsand T, Shakibaie M R. (2015). 'Anti-biofilm activity of biogenic selenium nanoparticles and selenium dioxide against clinical isolates of *Staphylococcus aureus*, P*seudomonas aeruginosa*, and *Proteus mirabilis'*, *Journal of Trace Elements in Medicine and Biology*, 29: 235-41.

Shareef AA, Hassan ZA, Kadhim MA, Al-Mussawi AA. (2022). 'Antibacterial Activity of Silver Nanoparticles Synthesized by Aqueous Extract of Carthamus oxycantha M. Bieb. Against Antibiotics Resistant Bacteria', *Baghdad Science Journal*, 19: 0460-60.

Siddique MH, Aslam B, Imran M, Ashraf A, Nadeem H, Hayat S, Khurshid M, Afzal M, Malik IR, Shahzad M. (2020). 'Effect of silver nanoparticles on biofilm formation and EPS production of multidrug-resistant Klebsiella pneumoniae', *BioMed Research International*, 2020: 6398165.

Soliman MKY, Hashem AH, Al-Askar AA, AbdElgayed G, Salem SS. (2024). 'Green synthesis of silver nanoparticles from Bauhinia variegata and their biological applications', *Green Processing and Synthesis*, 13: 20240099.

Soliman MKY, Salem SS, Abu-Elghait M, Azab MS. (2023). 'Biosynthesis of silver and gold nanoparticles and their efficacy towards antibacterial, antibiofilm, cytotoxicity, and antioxidant activities', *Applied Biochemistry and Biotechnology*, 195: 1158-83.

Tuyen NNK, Huong QTT, Duy BT, Nam NTH, Hai ND, An H, Tinh NT, Khanh TN, Nhi TL , Ngan LT. (2023). 'Selenium microparticles decorated graphene oxide via green synthesis using *Psidium guajava* leaves: preparation, characterization, and biological activities', *New Journal of Chemistry*, 47: 16993-7006.

Xu L, Xu M, Wang R, Yin Y, Lynch I, Liu S. (2020). 'The crucial role of environmental coronas in determining the biological effects of engineered nanomaterials', *Small*, 16: 2003691.

Yang B, Chen Y, Shi J. (2019). 'Reactive oxygen species (ROS)-based nanomedicine', *Chemical reviews*, 119: 4881-985.

Yousefi M, Pourmand MR, Fallah F, Hashemi A, Mashhadi R, Nazari-Alam A. (2016). 'Characterization of *Staphylococcus aureus* biofilm formation in urinary tract infection', *Iranian journal of public health*, 45: 485.

Zaki AG, Hasanien YA, El-Sayyad GS. (2022). 'Novel fabrication of SiO2/Ag nanocomposite by gamma irradiated Fusarium oxysporum to combat Ralstonia solanacearum', *AMB Express*, 12: 25.

Zambonino MC, Quizhpe EM, Jaramillo FE, Rahman A, Vispo NS, Jeffryes C, Dahoumane SA. (2021). 'Green synthesis of selenium and tellurium nanoparticles: current trends, biological properties and biomedical applications', *International Journal of Molecular Sciences*, 22: 989.

Zhu W, Clark N, Patel JB. (2013). 'pSK41-like plasmid is necessary for Inc18-like vanA plasmid transfer from Enterococcus faecalis to *Staphylococcus aureus* in vitro', *Antimicrobial agents and chemotherapy*, 57: 212-19.

Zoidis E, Seremelis I, Kontopoulos N, Danezis GP. (2018). 'Selenium-dependent antioxidant enzymes: Actions and properties of selenoproteins', *Antioxidants*, 7: 66.

Zonaro E, Lampis S, Turner RJ, Qazi SJS, Vallini G. (2015). 'Biogenic selenium and tellurium nanoparticles synthesized by environmental microbial isolates efficaciously inhibit bacterial planktonic cultures and biofilms', *Frontiers in microbiology*, 6: 584.